Electronic Supplementary Material (ESI) for Journal of Materials Chemistry C.
This journal is © The Royal Society of Chemistry 2019

Electronic Supplementary Information (ESI)

Centric-to-Acentric Structure Transformation Induced by Stereochemically Active Lone Pair: A New Insight for Design of IR Nonlinear Optical Materials

Hua Lin,[a] Yan-Yan Li,[b] Meng-Yue Li, [a] Zuju Ma,[,c] Li-Ming Wu[*, d] Xin-Tao Wu[a] and Qi-Long Zhu[*,a]*

[a]*State Key Laboratory of Structural Chemistry, Fujian Institute of Research on the Structure of Matter, Chinese Academy of Sciences, Fuzhou, Fujian 350002, China*

[b]*Taishan Scholar Advantage and Characteristic Discipline Team of Eco Chemical Process and Technology, Key Laboratory of Eco-chemical Engineering, College of Chemistry and Molecular Engineering, Qingdao University of Science and Technology, Qingdao 266042, China*

[c]*School of Materials Science and Engineering, Anhui University of Technology, Maanshan, 243002, China*

[d]*Key Laboratory of Theoretical and Computational Photochemistry, Ministry of Education, College of Chemistry, Beijing Normal University, Beijing 100875, China*

To whom correspondence should be addressed. E-mail: zjma@outlook.com; wlm@bnu.edu.cn; qlzhu@fjirsm.ac.cn.

1. Experimental Section

1.1 Materials and Instruments

All reagents were obtained from commercial sources and used without further purification. La ingot (2N) was purchased from Hohhot Jinrui Rare Earth Co., Ltd., Cu shot (5N), Sb lump (5N), and S powder (5N) were purchased from Alfa-Aesar.

Note that the external oxide layer on the surface of La ingot required to be thoroughly scraped before using it as reagent. Powder X-ray diffraction (PXRD) analysis was carried out in a Rigaku Mini-Flex II powder diffractometer (Cu-K_α, λ = 1.5418 Å). The semi-quantitative energy dispersive X-ray (EDX, Oxford INCA) spectra were measured with a field emission scanning electron microscope (FESEM, JSM6700F). Solid-state UV–Vis–NIR diffuse reflectance spectrum was recorded on a Perkin-Elmer Lambda 950 UV–Vis spectrophotometer with $BaSO_4$ as the standard.

1.2 Synthesis

The compound La_2CuSbS_5 was prepared from the elements (elemental ratio La : Cu : Sb : S = 2 : 1 : 1 : 5) in a $BaCl_2$/CsBr (1 : 1) flux at 1273 K. The starting reactants were loaded in a glove-box into carbon-coated silica tubes that were subsequently evacuated to 10^{-3} Pa and sealed. The tubes were heated at 1273 K for 72 h, and then cooled at 3 K h^{-1} to 673 K, and later the computer-controlled furnace was shut off. The dark-red flake crystals of La_2CuSbS_5 (see Figure S1a) are easily isolated from the products by washing with distilled water and dried by ethanol. The composition La : Cu : Sb : S of approximately 2 : 1 : 1 : 5 was established by EDX with the use of a JSM-6700F SEM (see Figure S1b). The homogeneous La_2CuSbS_5 was obtained as analyzed by the PXRD patterns shown in Figure S1c. Title compounds are stable in air more than three months.

1.3 Single crystal X-ray Crystallography

The single-crystal diffraction data collections was taken on a Mercury CCD equipped with graphite-monochromated Mo-K_α radiation (λ = 0.71073 Å) at room-temperature.

The absorption correction was done[1] and the structure was solved by the direct methods and refined by the full-matrix least-square fitting on F^2 using the *SHELX–2014* software.[2] All of the non-hydrogen atoms were refined with anisotropic thermal parameters and the coordinates were standardized using *STRUCTURE TIDY*.[3] The refinement details are summarized in Table S1. The positional coordinates and isotropic equivalent thermal parameters are given in Table S2, and the slected bond distances are listed in Table S3.

2. Computational details

The DFT calculations have been performed using the *Vienna ab initio simulation package* (VASP)[4–6] with the Perdew-Burke-Ernzerhof (PBE)[7] exchange correlation functional. The projected augmented wave (PAW)[8] potentials with the valence states 3s and 3p for S, 4s and 3d for Cu, 5s and 5p for Sb, 6s and 5d for La, respectively, have been used. A Γ-centered 3×5×5 Monkhorst-Pack grid for the Brillouin zone sampling[9] and a cutoff energy of 500 eV for the plane wave expansion were found to get convergent lattice parameters. Both the cell and atomic relaxations were carried out until the residual forces are below 0.02 eV/Å. A Monkhorst-Pack k-point mesh6 of 5×9×9 was used for the calculation of the linear and nonlinear optical properties. To better describe the exchange–correlation effects of localized electrons, a hybrid functionals (HSE06)[10] was used for the electronic structure calculations. The spin-polarization was considered in all calculations.

The imaginary part of the dielectric function due to direct inter-band transitions is given by the expression:

$$\varepsilon_2(\hbar\omega) = \frac{2e^2\pi}{\Omega\varepsilon_0}\sum_{k,v,c}\left|\left\langle\psi_k^c\left|u\cdot r\right|\psi_k^v\right\rangle\right|^2\delta(E_k^c - E_k^v - E) \quad \ldots\ldots\ldots\ldots (1)$$

Where Ω, ω, u, v and c are the unit-cell volume, photon frequencies, the vector defining the polarization of the incident electric field, valence and conduction bands, respectively. The real part of the dielectric function is obtained from ε_2 by a Kramers-Kronig transformation:

$$\varepsilon_1(\omega) = 1 + (\frac{2}{\pi})\int_0^{+\infty} d\omega' \frac{\omega'^2\varepsilon_2(\omega)}{\omega'^2 - \omega^2} \quad \ldots\ldots\ldots\ldots (2)$$

The refractive index $n(\omega)$ can be obtained based on ε_1 and ε_2.

In calculation of the static $\chi^{(2)}$ coefficients, the so-called length-gauge formalism derived by Aversa and Sipe[11] and modified by Rashkeev et al[12] is adopted, which has been proved to be successful in calculating the second order susceptibility for semiconductors and insulators.[13–16] In the static case, the imaginary part of the static second-order optical susceptibility can be expressed as:

$$\chi^{abc} = \frac{e^3}{\hbar^2\Omega}\sum_{nml,k}\frac{r_{nm}^a(r_{ml}^b r_{ln}^c + r_{ml}^c r_{ln}^b)}{2\omega_{nm}\omega_{ml}\omega_{ln}}[\omega_n f_{ml} + \omega_m f_{ln} + \omega_l f_{nm}]$$
$$+\frac{ie^3}{4\hbar^2\Omega}\sum_{nm,k}\frac{f_{nm}}{\omega_{mn}^2}[r_{nm}^a(r_{mn;c}^b + r_{mn;b}^c) + r_{nm}^b(r_{mn;c}^a + r_{mn;a}^c) + r_{nm}^c(r_{mn;b}^a + r_{mn;a}^b)]$$

……(3)

where r is the position operator, $\hbar\omega_{nm} = \hbar\omega_n - \hbar\omega_m$ is the energy difference for the bands m and n, $f_{mn} = f_m - f_n$ is the difference of the Fermi distribution functions, subscripts a, b, and c are Cartesian indices, and $r^b_{mn;a}$ is the so-called generalized derivative of the coordinate operator in k space,

$$r^{b}_{nm;a} = \frac{r^{a}_{nm}\Delta^{b}_{mn} + r^{b}_{nm}\Delta^{a}_{mn}}{\omega_{nm}} + \frac{i}{\omega_{nm}} \times \sum_{l} (\omega_{lm} r^{a}_{nl} r^{b}_{lm} - \omega_{nl} r^{b}_{nl} r^{a}_{lm}) \quad \text{..... (4)}$$

where $\Delta^{a}_{nm} = (p^{a}_{nn} - p^{a}_{mm}) / m$ is the difference between the electronic velocities at the bands n and m.

As the nonlinear optical coefficients is sensitive to the momentum matrix, much finer k-point grid and large amount of empty bands are required to obtain a convergent $\chi^{(2)}$ coefficient. The $\chi^{(2)}$ coefficients here were calculated from PBE wavefunctions with a 5×9×9 k-point grid and about 260 empty bands. A scissor operator has been added to correct the conduction band energy (corrected to the experimental gap), which has been proved to be reliable in predicting the second order susceptibility for semiconductors and insulators.[17–19]

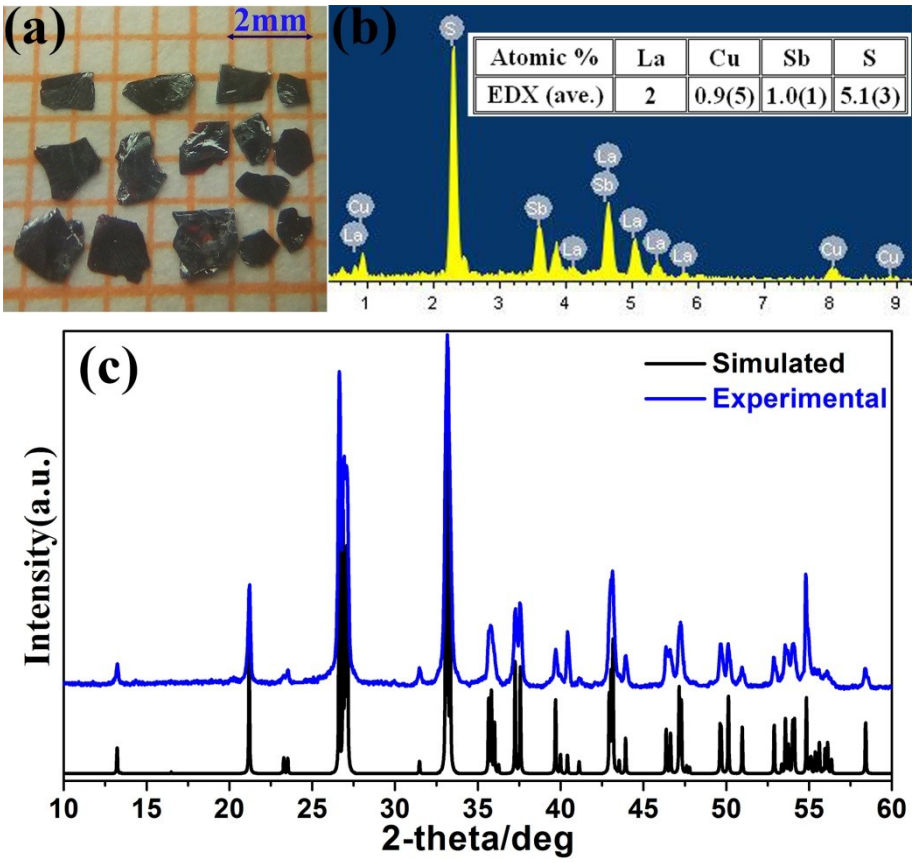

Figure S1. The characterizations of La_2CuSbS_5: (a) the photograph of crystals, (b) EDX results; and (c) PXRD patterns.

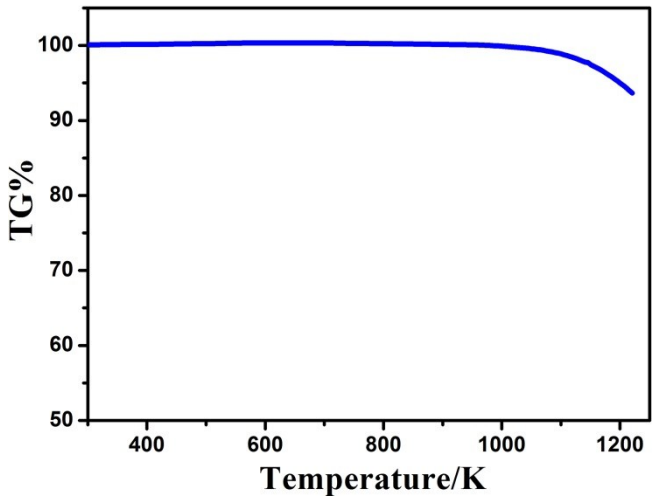

Figure S2. The TG curve of La_2CuSbS_5.

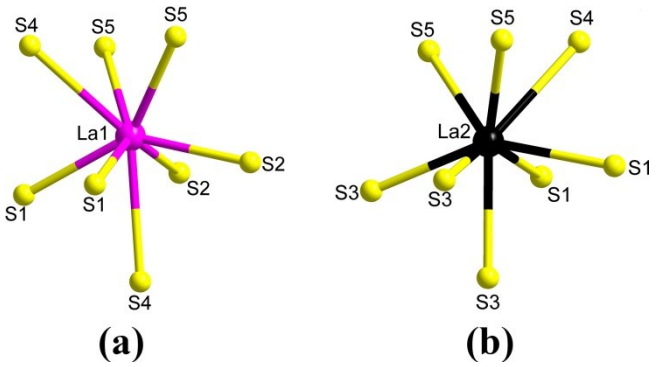

Figure S3. The local coordination environment of (a) La1 and (b) La2 atoms in La_2CuInS_5.

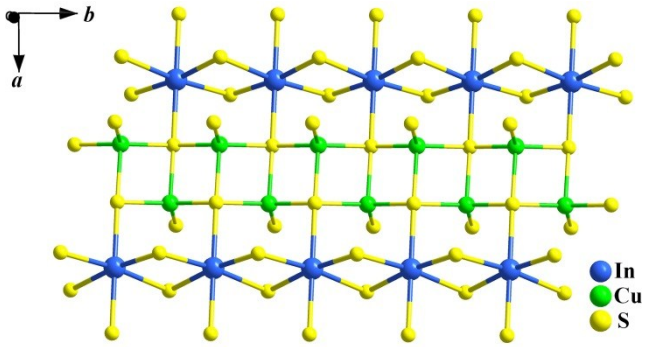

Figure S4. The 1D $\{[CuSbS_5]^{6-}\}_n$ chain in La_2CuInS_5.

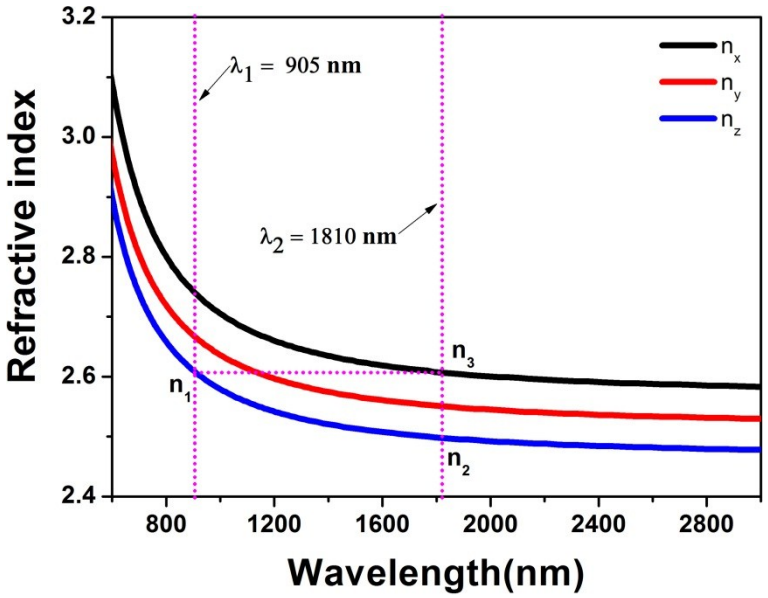

Figure S5. Phase-matching capabilities for La_2CuSbS_5 at 1810 nm. The minimum refractive index at 905 nm (n_1) located between the minimum (n_2) and maximum refractive index (n_3) at 1810 nm indicates the fulfillment of the requirement of the phase-matching condition.

Table S1. Crystallographic data and refinement details for La_2CuSbS_5.

Empirical formula	La_2CuSbS_5
Formula weight	623.41
Temperature(K)	293(2)
Crystal system	Orthorhombic
Space group	*Ima*2 (No.46)
a (Å)	13.382(6)
b (Å)	7.558(3)
c (Å)	7.635(3)
V (Å^3)	772.1(5)
Z	4
D_c (g·cm^{-3})	5.36
μ (mm^{-1})	18.27
GOOF on F^2	1.092
R_1, wR_2 ($I > 2\sigma(I)$) [a]	0.0439, 0.1145
R_1, wR_2 (all data)	0.0444, 0.1147
Largest diff. peak and hole (e·Å^{-3})	3.527, –2.741

[a]: $R_1 = \Sigma||F_o| - |F_c||/\Sigma|F_o|$, $wR_2 = [\Sigma w(F_o^2 - F_c^2)^2/\Sigma w(F_o^2)^2]^{1/2}$

Table S2. Atomic coordinates and equivalent isotropic displacement parameters of La_2CuSbS_5.

Atom	*Wyckff*	*x*	*y*	*z*	U_{eq}(Å)[a]
La1	4*a*	0	0	0.0011(2)	0.0115(4)
La2	4*b*	0.25	0.1341(2)	0.3864(3)	0.0117(4)
Cu	4*a*	0	0	0.5400(8)	0.054(2)
Sb	4*b*	0.25	0.6716(3)	0.2188(3)	0.016(5)
S1	4*b*	0.25	0.508(2)	0.502(2)	0.019(2)
S2	8*c*	0.1054(4)	0.3197(7)	0.1744(6)	0.011(2)
S3	8*c*	0.6037(4)	0.1644(7)	0.3295(7)	0.010(2)

U_{eq} is defined as one third of the trace of the orthogonalized U_{ij} tensor.

Table S3. Selected bond lengths (Å) of La_2CuSbS_5.

La1–S2 ×2	3.095(5)	La2–S2 ×2	2.886(5)
La1–S3 ×2	3.123(5)	La2–S2 ×2	2.950(5)
La1–S2 ×2	3.172(5)	La2–S1	2.961(8)
La1–S3 ×2	3.174(5)	La2–S3 ×2	3.019(6)
La1–S1 ×2	3.346(2)	La2–S1	3.130(2)
Cu–S2 ×2	2.214(6)	Sb–S3 ×2	2.467(6)
Cu–S3 ×2	2.460(7)	Sb–S1	2.486(2)
		Sb–S1	2.934(9)

Table S4. SHG intensities comparison of the well-known IR-NLO sulfides in recent

years at the same measured wavelength (λ = 2050 nm).

Compounds	SHG	LIDT	Ref.
$SnGa_4S_7$	1.3 × AGS	19 × AGS	20
Li_2ZnSiS_4	1.1 × AGS	10 × AGS	21
$Na_2ZnGe_2S_6$	0.9 × AGS	6 × AGS	22
Li_2BaSnS_4	0.7 × AGS	6.5 × AGS	23
Li_2BaGeS_4	0.5 × AGS	11 × AGS	23
$Ba_6Zn_7Ga_2S_{16}$	0.5 × AGS	28 × AGS	24
$BaAl_4S_7$	0.5 × AGS	10 × AGS	25
Li_2MnGeS_4	0.5 × AGS	40 × AGS	26
Na_2BaSnS_4	0.5 × AGS	5 × AGS	27
Na_2BaGeS_4	0.3 × AGS	8 × AGS	27
La_2CuSbS_5	**0.5 × AGS**	**6.7 × AGS**	**This work**
$AgGaS_2$(AGS)	1.0 × AGS	1.0 × AGS	28

REFERENCES

[1] *Crystal Clear*, version 1.3.5; Rigaku Corp.: The Woodlands, TX, **1999**.

[2] G. M. Sheldrick, *Acta Crystallogr., Sect. A: Found. Crystallogr.* **2008**, 112–122.

[3] L. M. Gelato and E. Parthe, *J. Appl. Crystallogr.* **1987**, **20**, 139–143.

[4] G. Kresse, VASP, 5.3.5; http://cms.mpi.univie.ac.at/vasp/vasp/vasp.html, **2014**.

[5] G. Kresse, J. Furthmuller, *Phys. Rev. B: Condens. Matter* **1996**, *54*, 11169–11186.

[6] G. Kresse, D. Joubert, *Phys. Rev. B: Condens. Matter* **1999**, *59*, 1758–1775.

[7] J. P. Perdew, K. Burke, M. Ernzerhof, *Phys. Rev. Lett.* **1996**, *77*, 3865–3868.

[8] P. E. Blochl, *Phys. Rev. B: Condens. Matter* **1994**, *50*, 17953–17979.

[9] H. J. Monkhorst, J. D. Pack, *Phys. Rev. B: Condens. Matter* **1976**, *13*, 5188.

[10] J. Heyd, G. E. Scuseria, M. Ernzerhof, *J. Chem. Phys.* **2003**, *118*, 8207–8215.

[11] C. Aversa, J. E. Sipe, *Phys. Rev. B* **1995**, *52*, 14636–14645.

[12] S. N. Rashkeev, W. R. L. Lambrecht, B. Segall, *Phys. Rev. B* **1998**, *57*, 3905.

[13] J. Hu, Z. Ma, J. Li, C. He, Q. Li, K. Wu, *J. Phys. Appl. Phys.* **2016**, *49*, 85103–85103.

[14] J. Li, Z. Ma, C. He, Q. Li, K. Wu, *J. Mater. Chem. C* **2016**, *4*, 1926–1934.

[15] Z. Ma, K. Wu, R. Sa, K. Ding, Q. Li, *Aip Advances* **2012**, *2*, 032170.

[16] Z. Ma, K. Wu, R. Sa, Q. Li, Y. Zhang, *J. Alloy. Compd.* **2013**, *568*, 16–20.

[17] B. Champagne, D. M. Bishop, *Adv. Chem. Phys.* **2003**, *126*, 41–92.

[18] A. H. Reshak, S. Auluck, I. V. Kityk, *Phys. Rev. B* **2007**, *75*, 245120.

[19] Y.-Z. Huang, L.-M. Wu, X.-T. Wu, L.-H. Li, L. Chen, Y.-F. Zhang, *J. Am. Chem. Soc.* **2010**, *132*, 12788–12789.

[20] Z. Z. Luo, C. S. Lin, H. H. Cui, W. L. Zhang, H. Zhang, Z. Z. He and W. D. Cheng, *Chem. Mater.*, **2014**, *26*, 2743–2749.

[21] G. M. Li, Y. Chu and Z. X. Zhou, *Chem. Mater.*, **2018**, *30*, 602–606.

[22] G. M. Li, K. Wu, Q. Liu, Z. H. Yang and S. L. Pan, *J. Am. Chem. Soc.*, **2016**, *138*, 7422–7428.

[23] K. Wu, B. B. Zhang, Z. H. Yang and S. L. Pan, *J. Am. Chem. Soc.*, **2017**, *139*, 14885–14888.

[24] Y. Y. Li, P. F. Liu and L. M. Wu, *Chem. Mater.*, **2017**, *29*, 5259–5266.

[25] D. J. Mei, J. Q. Jiang, F. Liang, S. Y. Zhang, Y. D. Wu, C. T. Sun and Z. S. Lin, *J. Mater. Chem. C*, **2018**, *6*, 2684–2689.

[26] J. A. Brant, D. J. Clark, Y. S. Kim, J. I. Jang, A. Weiland and J. A. Aitken, *Inorg. Chem.*, **2015**, *54*, 2809–2819.

[27] K. Wu, Z. H. Yang and S. L. Pan, *Angew. Chem. Int. Ed.*, **2016**, *55*, 6713–6715.

[28] A. Harasaki and K. Kato, *Jpn. J. Appl. Phys*., **1997**, *36*, 700–703.